Title
Inducible Renitence Limits Listeria monocytogenes Escape from Vacuoles in Macrophages

Journal
The Journal of Immunology, 189(9)

ISSN
0022-1767

Authors
Davis, Michael J
Gregorka, Brian
Gestwicki, Jason E
et al.

Publication Date
2012-11-01

DOI
10.4049/jimmunol.1103158

Peer reviewed

Published in final edited form as:
J Immunol. 2012 November 1; 189(9): 4488–4495. doi:10.4049/jimmunol.1103158.

Inducible Renitence limits *Listeria monocytogenes* Escape from Vacuoles in Macrophages

Michael J. Davis[*], **Brian Gregorka**[†], **Jason E. Gestwicki**[‡], and **Joel A. Swanson**[*,†,2]

[*]Graduate Program in Immunology, University of Michigan Medical School, Ann Arbor, MI 48109-5620

[†]Department of Microbiology and Immunology, University of Michigan Medical School, Ann Arbor, MI 48109-5620

[‡]Life Sciences Institute. University of Michigan, Ann Arbor, MI 48109, U.S.A

Abstract

Membranes of endolysosomal compartments in macrophages are often damaged by physical or chemical effects of particles ingested through phagocytosis or by toxins secreted by intracellular pathogens. This study identified a novel inducible activity in macrophages which increases resistance of phagosomes, late endosomes and lysosomes to membrane damage. Pretreatment of murine macrophages with lipopolysaccharide, peptidoglycan, tumor necrosis factor-α or interferon-γ (IFN-γ) conferred protection against subsequent damage to intracellular membranes caused by photooxidative chemistries or by phagocytosis of ground silica or silica microspheres. Phagolysosome damage was partially dependent on reactive oxygen species, but was independent of the phagocyte oxidase. IFN-γ-stimulated macrophages from mice lacking the phagocyte oxidase inhibited escape from vacuoles by the intracellular pathogen *Listeria monocytogenes (L.m.)*, which suggested a role for this inducible renitence (resistance to pressure) in macrophage resistance to infection by pathogens that damage intracellular membranes. Renitence and inhibition of *L.m.* escape were partially attributable to heat shock protein-70 (HSP70). Thus, renitence is a novel, inducible activity of macrophages which maintains or restores the integrity of endolysosomal membranes.

Introduction

Classical macrophage activation in response to lipopolysaccharide (LPS), other bacteria-derived molecules and the cytokines IFN-γ and TNF-α, is important in host defense against infections (1, 2), as well as in sepsis, cancer and atherosclerosis (3–5). Induced biochemical activities which counteract infection include the phagocyte NADPH oxidase (6) and inducible nitric oxide synthase (7), which generate toxic reactive oxygen species (ROS) and reactive nitrogen species (RNS), respectively. Other antimicrobial activities include increased phagosome-lysosome fusion, antigen presentation, iron sequestration, and autophagy (8–10). Bacterial infection of macrophages also increases cellular expression of HSP70, which can be released from macrophages through non-classical secretion systems (11, 12). Only a fraction of the activation-regulated genes have been implicated in these processes (13), which suggests the existence of other activities which macrophages use to combat infection.

[2]corresponding author: Joel A. Swanson, Department of Microbiology and Immunology, University of Michigan Medical School, Ann Arbor, MI 48109-5620, Tel: 734-647-6339, Fax: 734-764-3562, jswan@umich.edu.

Classical macrophage activation was originally identified from the ability of a sub-lethal infection with *Listeria monocytogenes*(*L.m.*) to protect mice from subsequent infectious challenges (14). *L.m.* is a Gram-positive facultative intracellular pathogen which causes gastrointestinal disease or more serious infections in pregnant women, neonates or immuno-compromised individuals (15). After entry into cells by phagocytosis, *L.m.* secretes a cholesterol-dependent cytolysin, lysteriolysin O (LLO), which facilitates escape from macrophage phagosomes into the cytosol. Bacteria typically escape macrophage phagosomes prior to phagosome-lysosome fusion (16). Wildtype *L.m.,* but not *L.m.* lacking LLO (Δ*hly*), can disrupt pH and calcium gradients across phagosomal membranes, which delays fusion of phagosomes containing bacteria with LAMP-1-positive lysosomes (16, 17). In the cytosol, *L.m.* multiplies and eventually co-opts the host actin cytoskeleton to invade neighboring cells. Activation of macrophages by IFN-γ has a critical role in protecting mice from *L.m.* infection (18), significantly altering the dynamics of *L.m.* in macrophages (19, 20). Reactive oxygen and nitrogen species produced by activated macrophages inhibit *L.m.* infection and escape from the macrophage phagosome (21, 22). The roles of other functions of activated macrophages in preventing *L.m.* escape remain unknown.

In a previous study of lysosome damage, we determined that the phagolysosomes of mouse macrophages treated with LPS were more resistant to damage after phagocytosis of ground silica or silica microspheres (SMS) than were phagolysosomes of unstimulated macrophages (23). Earlier studies indicated roles for HSP70 in stabilizing lysosomes (24–28). As damage to endocytic compartment membranes is a necessary consequence of infections by intracellular pathogens which access host cell cytosol, increased resistance to such membrane-damaging activities would be a novel mechanism of resistance to infection. We therefore examined the mechanism of this novel inducible activity and the contribution of HSP70 to that resistance. We show that the protective effect could be induced by Toll-like receptor ligands, IFN-γ, TNF-α, intact bacteria and exogenously added HSP70. This activity limited damage from a variety of agents including ground silica, silica microspheres, light-induced membrane damage and infection by *L.m.*, indicating it as a general protective response of activated macrophages.

Materials and methods

Materials

Fluorescein-dextran (Fdx) avg. mol. wt. 3000 Daltons, RPMI 1640, fetal calf serum (FCS), penicillin/streptomycin solution, valinomycin, nigericin, recombinant mouse IL-10, recombinant mouse IL-1β, SNARF-1 carboxylic acid acetate succinimidyl ester, Cell trace CFSE cell proliferation kit (carboxyfluorescein diacetate succinimidyl ester), Texas red-dextran average molecular weight 10,000 Daltons (TRdx), Texas red-phalloidin, and gentamicin solution were purchased from Invitrogen (Carlsbad, CA, USA). Recombinant human IFN-β, diphenyleneiodonium (DPI) and n-acetyl-l-cystiene (NAC), were purchased from Sigma Chemical Co. (St. Louis, MO. USA). Lipopolysaccharide #225 *Salmonella typhurium* was from List Biological Laboratories INC (Campbell, CA, USA). 35 mm dishes with attached 14 mm coverglass were purchased from MatTek Corp (Ashland, MA, USA). Peptidoglycan (PGN) from *Escherichia coli* 0111:B4 was purchased from Invivogen (San Diego, CA, USA). IFN-γ was from R&D Systems (Minneapolis, MN, USA), TNF-α was from eBiosciences (San Diego, CA, USA) and murine IL-6 was from Calbiochem (San Diego, CA, USA). MIN-U-SIL-15 ground silica was a gift from U.S. Silica (Berkeley Springs, WV, USA). Oxide silica 3 μm microspheres (SMS; Microspheres-Nanospheres, Cold Spring, NY, USA) were washed overnight in 1 N HCl then rinsed several times in distilled water. For some experiments, SMS were coated with 0.1 M poly-L-lysine (PLL) for 30 minutes. Recombinant HSP70 and HSC70 were purified as in ref. (29). The synthesis of Ym1 (a.k.a. MKT077) has been described (30).

Bone marrow-derived macrophages

C57BL/6J (wildtype), B6.129S-*Cybb*^{tm1Din}/J (Nox-2 deficient) and TLR4 −/− mice (strain C57BL6/10SCN) were purchased from Jackson Labs (Bar Harbor, ME, USA). All mice were maintained under specific pathogen-free conditions at the University of Michigan animal facility. Differentiation of macrophages from mouse bone marrow cells has been previously described (23, 31). Briefly, marrow cells extracted from mouse femurs were cultured for six days in the presence of M-CSF, which was provided by 30% L-cell-conditioned medium. Bone marrow-derived macrophages (BMM) were frozen and stored at −130° C as aliquots in M-CSF-containing medium with 10% DMSO and thawed as needed for experiments.

Loading macrophage lysosomes and stimulation of cells

After allowing BMM to attach for several hours in RPMI 1640 with 10% FCS and penicillin/streptomycin, cells were incubated overnight in medium containing 150 μg/mL Fdx. BMM were then rinsed and chased in unlabeled medium for at least 3 hours to allow Fdx trafficking into late compartments of the endolysosomal network (32). Penicillin/streptomycin was omitted from BMM cultures to be infected with *L.m.* LPS (100 ng/mL), PGN (2.5 μg/mL), IFN-γ (100 U/mL), TNF-α (100 ng/mL), IL-6 (5 ng/mL), IL-10 (100 ng/mL), IL-1β (10 ng/mL) or IFN-β (100 U/mL) were included in both the Fdx pulse medium and the subsequent Fdx-free chase medium. Uncoated SMS were fed to BMM in serum-free medium or PLL-coated SMS were fed to cells in medium containing 10% FCS and incubated 1 hr before imaging.

Measurement of damage to endolysosomal compartments

Endolysosomal membrane damage was measured in live BMM by epi-fluorescence ratiometric microscopy, as described previously (23). Cells loaded with Fdx were rinsed and imaged in Ringer's buffer (155 mM NaCl, 5 mM KCl, 2 mM $CaCl_2$, 1 mM $MgCl_2$, 2 mM NaH_2PO_4, 10 mM Hepes, and 10 mM glucose), using a Nikon TE300 inverted microscope equipped with a mercury arc lamp, 60× plan-apochromat 1.4-numerical aperture objective, a cooled digital CCD camera (Quantix Photometrics, Tucson, AZ, USA), a temperature-controlled stage and a Fura/FITC ratiometric dichroic mirror (Omega Optical, Brattleboro, VT, USA). Three images were acquired for each field of cells: one phase-contrast image and two fluorescence images, which used a 510 nm emission filter and two different excitation band pass filters (centered at 440 nm and 485 nm), mounted in computer-controlled filter wheels (Sutter Instruments, Novato, CA, USA). Metamorph software (Molecular Devices, Downingtown, PA, USA) was used for image capture and analysis.

The Fdx signal in the 440 nm excitation channel is relatively insensitive to pH, whereas the signal in the 485 excitation channel varies between pH 4.5 and 7.5. Thus, the ratio of Fdx fluorescence in the 485 nm channel divided by that in the 440 nm channel is related to pH in any sub-region of an image (pixel). For calibration, 485 nm /440 nm excitation ratios were measured in cells with intracellular pH fixed at pH 9.0, 7.5, 7.0, 6.5, 6.0, 5.5, 5.0, 4.5 and 4.0, using ionophores nigericin and valinomycin (10 μM) in clamping buffers (130 mM KCl, 1 mM $MgCl_2$, 15 mM Hepes, 15 mM MES). Ratios were converted to pH, as described previously (17, 23, 33). A 4-variable sigmoidal standard curve was then constructed using Sigmaplot software (San Jose, CA, USA). Regions showing pH greater than pH 5.5 were taken to indicate lysosome release. The percent of Fdx released in cells was calculated by summing the 440 nm intensity of pixels in regions of pH above 5.5 and dividing this value by the summed 440 nm intensity for the entire cell.

Photo-oxidative damage of lysosomes

BMM were co-loaded with 150 μg/mL Fdx along with 75 μg/mL TRdx, then stimulated with LPS and IFN-γ for 18 hrs, as described above. TRdx was used as a photosensitizer and Fdx imaging was used to monitor lysosome damage. BMM were rinsed with Ringer's buffer, mounted onto the microscope heated stage, and allowed to equilibrate for 5 min. A field was selected for imaging, then an initial Fdx image set was acquired. Using a 580 nm TRdx excitation filter, cells were then exposed to bright light in regular, 5-sec exposures. Between each exposure, Fdx images at 440 nm and 485 nm were acquired to assess lysosome damage. This process was repeated for 60 total sec of 580 nm photo-exposure (12×5 sec). Percent Fdx release was then calculated from the Fdx images for each time point.

Infection of cells with *Listeria monocytogenes*

Wildtype *Listeria monocytogenes (L.m.)* strain (DP-L10403) and Δ*hly L.m.* (DP-L2161) were provided by Daniel Portnoy, University of California, Berkeley. *L.m.* cultures were grown overnight at room temperature then diluted and grown 75 minutes at 37 degrees with shaking to O.D. 600nm = 0.8. One mL of bacterial culture was then centrifuged (2 min at 5000×g) and resuspended in Ringer's buffer. Bacteria were stained using SNARF-1 or CFSE dye for 15 min in a shaking 37° C incubator. The culture was then washed three times in Ringer's buffer. BMM were infected by adding bacteria to 200 μL of culture medium without antibiotics and replacing the BMM culture medium with this infection mix. All infections were 10 minutes followed by rinsing in Ringer's buffer and chasing in culture medium containing gentamicin. After 90–120 min of culture, infected cells were either imaged for damage or fixed to measure *L.m.* escape.

Measurement of vacuole escape by *Listeria monocytogenes*

BMM infected with CFSE-stained *L.m.* were fixed using cytoskeleton fix (2% paraformelahyde, 30mM Hepes, 10mM EGTA, 0.5 mM EDTA, 5 mMMgSO4, 33 mM potassium acetate, 5% polyethylene glycol 400) and permeabilized in 0.1% Triton X-100 in PBS. Coverslips were blocked in PBS containing 2% goat serum and stained using Texas Red-phalloidin and DAPI. Cells were imaged and the numbers of total (DAPI-positive) and escaped (Texas Red-phalloidin-positive) bacteria was recorded for each infected macrophage.

Immunofluorescence Microscopy

BMM on 12 mm circular coverslips were stimulated overnight with IFN-γ or LPS, then prepared for immunofluorescence microscopy. Cells were fixed for 60 min at 37°C (Fixative: 2% paraformaldehyde, 4.5% sucrose, 20 mM HEPES, pH 7.4, 70 mM NaCl, 10 mM KCl, 10 mM $MgCl_2$, 2 mM EGTA, 70 mM lysine-HCl, 10 mM sodium periodate), rinsed (TBS: 20 mM Tris-HCl, pH 7.4, 4.5% sucrose, 150 mM NaCl), extracted with −20°C methanol, rinsed with TBS+2% sheep serum (TSS), incubated with primary antibodies against HSP70 (rabbit anti-HSP70/HSC70; Santa Cruz Biotechnology) and LAMP-1 (rat monoclonal 1D4B; Developmental Studies Hybridoma Bank, Iowa City, IA) in TSS, rinsed with TSS, incubated with secondary antibodies (AlexaFluor488-labeled Goat anti-Rat IgG; AlexaFluor594-labeled Goat anti-Rabbit IgG; Invitrogen), rinsed, mounted in anti-fade and observed by digital fluorescence microscopy. The fluorescence of Alexa488-labeled HSP70 was quantified from digital images of 10 cells for each condition.

Statistical methods

Student's T-Test was performed on groups of cells containing similar amounts of SMS, *L.m.* or photostimulation.

Results

Macrophage activation stabilizes lysosomes

Previous studies established that particle-mediated lysosome damage was reduced after macrophages were stimulated with LPS (23). To determine which other agents could induce this effect, BMM late endosomes and lysosomes were loaded with Fdx and stimulated with cytokines or Toll-like receptor (TLR) ligands, then the damage induced by phagocytosis of silica microspheres (SMS) was measured as the release of Fdx from endolysosomal compartments into cytoplasm (Fig. 1A, B). LPS, PGN, IFN-γ, and TNF-α protected endolysosomes from SMS challenge, whereas IL-6, IL-10, IL-1β, and IFN-β did not. Time-course measurements indicated that full lysosome protection required 18 hrs of LPS stimulation, although significant protection was observed after five hrs (Fig. 1C). We termed this inducible membrane resistance or repair mechanism renitence: resistance to pressure.

The studies of Mackaness which first described a role for activated macrophages in host defense showed that infection of mice with sublethal doses of *L.m.* led to differentiation of macrophages with increased resistance to subsequent *L.m.* infections (14). Although activation was eventually attributed to the action of IFN-γ and TNF-α (34), we postulated that some of the increased resistance may be induced directly by bacteria. We therefore measured the extent to which phagocytosis of hemolysin-deficient (Δ*hly*) *L.m.*,, which do not damage vacuoles (17, 35, 36), increased macrophage resistance to subsequent challenge by phagocytosed SMS. BMM which ingested Δ*hly L.m.* became resistant to lysosome damage after phagocytosis of SMS (Fig. 1D). The subset of BMM which were exposed to Δ*hly L.m.* but which did not ingest bacteria showed lysosome damage levels comparable to unstimulated cells (Fig. 1E), indicating that the Δ*hly L.m.* activated this protective mechanism inside the cells that ingested them, rather than through some secreted factor. This suggests that microbes ingested by macrophages initiate a cytokine-independent differentiation to a more resistant phenotype.

Reactive oxygen species contribute to particle-mediated lysosome damage

Inducible renitence could interfere with the mechanism(s) by which particles damage membranes. As ROS have been implicated in NLRP3 inflammasome activation by lysosome damage (37, 38), we examined the contribution of ROS to phagolysosome damage. Macrophages were pretreated with diphenyleneiodonium (DPI), which is a potent inhibitor of ROS-generating activities in macrophages, including the phagocyte oxidase (NOX2) and the mitochondrial electron transport chain (39–41). Macrophages loaded with Fdx and incubated in DPI or control medium were fed ground silica or SMS and the extent of damage was assessed. DPI reduced phagolysosome damage following phagocytosis of both kinds of particle (Figs. 2A, B). Similarly, BMM pre-incubated in the antioxidant n-acyl-cysteine (NAC) showed less SMS-mediated lysosome damage than did control cells (Fig. 2C). This reduced damage was independent of any DPI effect on the efficiency of phagocytosis, as DPI-treated BMM which had phagocytosed SMS showed less lysosome damage than control cells which had ingested equivalent numbers of particles. These data indicate that phagocyte oxidase-independent ROS contribute to silica-induced lysosome damage. Renitence may therefore consist of mechanisms which interfere with ROS generation in cytoplasm.

A major source of ROS in the phagosomal lumen is the phagocyte oxidase. We examined the contribution of phagocyte oxidase-generated ROS to damage by comparing wildtype and phagocyte oxidase (*nox2*)-deficient BMM and observed similar levels of phagolysosome damage following phagocytosis of ground silica (Fig. 2D) or SMS (Fig. 2E). This indicates that the phagocyte oxidase does not contribute to particle-mediated lysosome damage.

Listeria monocytogenes hemolysin damages endolysosomes

The relationship between *L.m.* vacuolar escape and endolysosome damage was investigated. A previous study suggested that at a low multiplicities of infection (MOI) *L.m.* escapes from LAMP-1-negative, late endosome-like vacuoles (16), which suggests that escape could occur without causing release of Fdx from late endocytic compartments. To determine if infection at higher MOI damages late endocytic compartments, Fdx-loaded BMM were fed SNARF-1-labeled wildtype or Δ*hly L.m.* and assayed for endolysosome damage. In cells containing fewer than seven bacteria, wildtype *L.m.* showed low levels of lysosome damage, consistent with a mechanism in which *L.m.* escapes from vacuoles at earlier stages of maturation. However, higher bacterial loads showed more damage, which correlated with the number of *L.m.* per BMM (Fig. 3 A-D). BMM infected with Δ*hly L.m.* showed neither lysosome damage nor *L.m.* escape, confirming that both activities required LLO. Thus, although at low MOI *L.m.* entered cytoplasm with negligible damage to late endocytic compartments, higher MOI resulted in LLO-dependent release of Fdx from those compartments into cytoplasm.

Inducible renitence inhibits *L.m.* escape and associated lysosome damage

The phagocyte oxidase inhibits *L.m.* escape in activated macrophages (21, 22). To determine if inducible renitence also contributes to the inhibition of *L.m.* escape in activated macrophages, wildtype and *nox2*-deficient BMM were loaded with Fdx, activated with IFN-γ, infected with wildtype *L.m.* and scored for actin-positive cytoplasmic bacteria. IFN-γ treatment limited *L.m.* escape in both wildtype and *nox2*-deficient BMM. Although IFN-γ-activated, *nox2*-deficient BMM did not inhibit escape as efficiently as IFN-γ-activated wildtype BMM, they were significantly better than unactivated, *nox2*-deficient BMM (Fig. 3E). IFN-γ-activated, *nox2*-deficient BMM also showed reduced levels of endolysosome damage after *L.m.*, infection compared to unactivated *nox2*-deficient cells (Fig. 3F). This Nox2-independent resistance suggests that inducible renitence inhibits *L.m.* escape from vacuoles of activated macrophages. However, contributions of other IFN-γ-inducible activities to macrophage resistance to *L.m.* escape cannot be excluded.

Inducible renitence protects lysosomes against photo-oxidative damage

Inducible renitence was also measured in a non-particulate endolysosome-damaging assay. Late endosomes and lysosomes were loaded by endocytosis with TRdx, as a photosensitizer, and Fdx, to monitor membrane integrity. Cells were stimulated with LPS or IFN-γ, then exposed to 580 nm light, which excites TRdx but not Fdx. The excited TRdx increases photo-oxidative chemistries which damage cell membranes (24, 42). Lysosome integrity was measured by imaging Fdx after each 580 nm exposure. In unstimulated BMM, lysosome damage was detectable after 25 sec exposure and was nearly complete by 50 secs (Fig. 4). Control BMM, in which endolysosomes were loaded with Fdx but not TRdx and exposed similarly to 580 nm light, showed no damage. Half-maximal lysosome damage in LPS- or IFN-γ-stimulated BMM required greater exposure to light than in unstimulated BMM (Fig. 4A & B), Thus, the inducible resistance to membrane damage also affects non-phagosomal lysosomes.

HSP70 limits damage

As infection can increase synthesis and secretion of HSP70 from macrophages (11, 12) and exogenously added HSP70 can increase lysosomal resistance to photodamage (24), we hypothesized that HSP70 contributed to induced renitence. Macrophages were incubated with recombinant HSP70 or LPS and endolysosome damage was measured after SMS phagocytosis. Exogenous HSP70 reduced lysosome damage to levels comparable to those in LPS-activated cells (Fig. 5A). To rule out endotoxin contamination as an alternative

explanation for HSP70-mediated lysosome protection (43), damage was measured in TLR4-deficient BMM. These cells showed significant resistance to damage when treated with recombinant HSP70 or IFN-γ but not with LPS (Fig. 5B, C). HSP70-mediated protection was also inhibited by the inhibitors of HSP70 ATPase activity Ym1 (30, 44) and Myr (29, 45, 46) (Fig 5B). HSC70 induced less protection than HSP70 (Fig. 5C), consistent with previous observations indicating the specificity of HSP70 for lysosome-protective effects (24). To test the hypothesis that endogenous HSP70 contributes to inducible lysosome renitence, macrophages were loaded with Fdx and stimulated with LPS for 0, 5 or 18 hrs. For the last 5 hrs before phagocytosis of SMS, cells were treated with HSP70 inhibitors Ym1 and Myr. Macrophages stimulated with LPS in the presence of inhibitors showed greater endolysosome damage than cells without drug (Fig. 5D), indicating that HSP70 mediates LPS-induced renitence. The contribution of HSP70 to inducible renitence was also tested in an *L.m.* infection model. TLR4-deficient BMM were treated with HSP70 or IFN-γ, infected with *L.m.* and scored for escape. HSP70-treated BMM showed a reduction in *L.m.* escape comparable to IFN-γ stimulated cells (Fig. 5E). Inhibitors of HSP70 partially reversed the IFN-γ-mediated reduction in *L.m.* vacuolar escape, indicating that HSP70-mediated membrane protection inhibits *L.m.*, vacuolar escape and that HSP70 contributes to inducible renitence.

Immunofluorescence microscopy indicated that total levels of HSP70 increased in BMM stimulated with LPS (Fig. 5F, G) and IFN-γ (data not shown) and that HSP70 localized to small, LAMP-1-negative vesicles. Lack of co-localization between HSP70 and LAMP-1 suggests that HSP70 effects on renitence do not occur from within the endolysosomal network.

Discussion

This study identifies inducible renitence as a novel common feature of classical macrophage activation, which can be induced by the TLR ligands LPS and PGN, by whole bacteria and by the cytokines IFN-γ and TNF-α. Renitence was observed in a variety of different membrane-damaging insults, including phagocytosis of ground or microsphere silica particles, LLO-dependent membrane perforation and photo-oxidative chemistries. Thus, inducible renitence is unlikely to involve mechanisms specific to any one kind of damage but instead represents a set of activities which reinforce endolysosomal membranes. Although the assays used here allowed us to analyze renitence as a feature of late endosomes and lysosomes, it is possible that other membranous compartments, such as early endosomes or endoplasmic reticulum, may exhibit renitence, as well. It will be interesting to determine if renitence is inducible in other common targets of infection, such as dendritic cells and epithelial cells.

Renitence was induced by mediators of classical activation in macrophages, indicating a role in inflammation and host defense against infections. Previous studies showed that resistance of lysosomes to various kinds of damage can be induced by LPS (23), TNF-α (47) or HSP70 (24), all of which are associated with infection. That infection by Δ*hly L.m.* could also induce renitence suggests that early signaling by TLRs induces renitence as a protection against subsequent infections. Local induction by Δ*hly L.m.* (Fig. 1E) suggests that at least some of the induction is cell autonomous. It remains to be determined if renitence is inducible by TLR signaling, by membrane damage itself or by bacterial HSP70 (ie., DnaK).

In cells containing low numbers of bacteria, *L.m.* escape occurred with negligible damage to late endosomes and lysosomes (Fig. 3D). As lysosomal perforation can activate inflammasomes (38), the escape of *L.m.* from pre-lysosomal compartments may function as an immune evasion strategy. Although macrophages containing few bacteria showed little

damage, cells containing many bacteria showed extensive endolysosomal damage, which suggests that the mechanisms which allow *L.m.* to escape prior to phagosome-lysosome fusion may break down later in infection when more bacteria are present in an area. LLO secreted by *L.m.*, prior to escape or *L.m.* into phagosomal vacuoles may be trafficked to later compartments and perforate membranes there. Alternatively, LLO secreted by cytosolic *L.m.* could damage lysosomal membranes.

The mechanisms underlying renitence remain unknown, but could include reduced susceptibility to membrane-damaging chemistries, increased resistance of membranes to damage or the upregulation of a membrane-repair process. Non-phagosomal ROS contributed to damage induced by silica particles (Fig. 2), and ROS generated in the lysosome lumen likely account for phototoxic damage by TRdx photo-stimulation (Fig. 4). Increased synthesis of glutathione was implicated in the TNF-α-induced resistance to lysosome damage (47), consistent with a role for cellular antioxidants in limiting damage. In cells infected with *L.m.*, phagosome-derived ROS inhibited escape of *L.m.* from the macrophage phagosome (21). Thus, while modulation of ROS remains a possible mechanism for limiting damage, this is unlikely to be the main mechanism of renitence. Decreased sensitivity to photodamage induced by LPS or IFN-γ (Fig. 4) indicated that endolysosomal membranes become more resistant to damage. The potential roles for membrane damage-repair mechanisms in renitence remain to be tested.

Vacuolar membrane damage can have significant physiological and immunological consequences. Aside from allowing access of microbes or virulence factors into cytoplasm, membrane damage induces a pro-inflammatory cell death program in macrophages (38). Lysosome damage is implicated in several diseases of crystal or particle accumulation, such as silicosis, arteriosclerosis, gout and asbestosis (37, 38, 48). Lysosome damage in unactivated cells results in non-inflammatory cell death (49). These different consequences in activated and non-activated cells may explain why renitence is an inducible activity. A low level of endocytic membrane leakage into cytoplasm (23, 50) may be beneficial in some circumstances, as it may allow surveillance by cytoplasmic Nod-like receptors (51) or facilitate the cross presentation of exogenous antigens on MHC class I molecules (52).

The mechanism of endolysosome protection by HSP70 is unknown. Bacterial infection of macrophages can lead to increased synthesis and secretion of HSP70 via non-classical routes, including exosomes (12). Exogenous HSP70 activates lysosomal acid sphingomyelinase which, in turn, catalyzes phospholipid chemistries that increase damage-resistance of lysosomal membranes in fibroblasts (24). The evidence presented here indicates that activated macrophages induce a similar state in their lysosomes (Fig. 5). HSP70 levels were increased by LPS and IFN-γ, but HSP70 did not localize to lysosomes. This suggests that the effect of HSP70 on renitence may be autocrine. As HSP70 inhibitors only partially reversed lysosome renitence induced by LPS (Fig. 5D) or IFN-γ (Fig. 5E), we hypothesize that HSP70-mediated protection is one of several membrane-stabilizing activities that comprise inducible renitence.

Thus, renitence is a novel pathway induced in activated macrophages which reduces damage to endolysosomal membranes caused by mechanical forces or by *L.m.* This suggests that therapeutic interventions which increase renitence could be efficacious against infection by intracellular pathogens or in reducing inflammation due to micro- or nano-particles.

Acknowledgments

We gratefully acknowledge Yoshinari Miyata for synthesis of Ym1.

Supported by NIH grants AI 035950 to J.A.S. and NS 059690 to J.E.G. M.J.D. was, in part, supported by NIH training grant T32 HL07749.

Literature Cited

1. Mosser DM, Edwards JP. Exploring the full spectrum of macrophage activation. Nat Rev Immunol. 2008; 8:958–969. [PubMed: 19029990]
2. Cassol E, Cassetta L, Rizzi C, Alfano M, Poli G. M1 and M2a polarization of human monocyte-derived macrophages inhibits HIV-1 replication by distinct mechanisms. J Immunol. 2009; 182:6237–6246. [PubMed: 19414777]
3. Lin WJ, Yeh WC. Implication of Toll-like receptor and tumor necrosis factor alpha signaling in septic shock. Shock. 2005; 24:206–209. [PubMed: 16135957]
4. Hallam S, Escorcio-Correia M, Soper R, Schultheiss A, Hagemann T. Activated macrophages in the tumour microenvironment-dancing to the tune of TLR and NF-kappaB. J Pathol. 2009; 219:143–152. [PubMed: 19662665]
5. Wilson HM. Macrophages heterogeneity in atherosclerosis - implications for therapy. J Cell Mol Med. 2010; 14:2055–2065. [PubMed: 20629993]
6. Nauseef WM. Biological roles for the NOX family NADPH oxidases. J Biol Chem. 2008; 283:16961–16965. [PubMed: 18420576]
7. MacMicking J, Xie Q-w, Nathan C. Nitric oxide and macrophage function. Annu. Rev. Immunol. 1997; 15:323–350. [PubMed: 9143691]
8. Trost M, English L, Lemieux S, Courcelles M, Desjardins M, Thibault P. The phagosomal proteome in interferon-gamma-activated macrophages. Immunity. 2009; 30:143–154. [PubMed: 19144319]
9. Cairo G, Recalcati S, Mantovani A, Locati M. Iron trafficking and metabolism in macrophages: contribution to the polarized phenotype. Trends Immunol. 2011; 32:241–247. [PubMed: 21514223]
10. Levine B, Mizushima N, Virgin HW. Autophagy in immunity and inflammation. Nature. 2011; 469:323–335. [PubMed: 21248839]
11. Pockley AG. Heat shock proteins as regulators of the immune response. Lancet. 2003; 362:469–476. [PubMed: 12927437]
12. Anand PK, Anand E, Bleck CK, Anes E, Griffiths G. Exosomal Hsp70 induces a pro-inflammatory response to foreign particles including mycobacteria. PLoS One. 2010; 5:e10136. [PubMed: 20405033]
13. Martinez FO, Gordon S, Locati M, Mantovani A. Transcriptional profiling of the human monocyte-to-macrophage differentiation and polarization: new molecules and patterns of gene expression. J Immunol. 2006; 177:7303–7311. [PubMed: 17082649]
14. Mackaness GB. Cellular resistance to infection. J. Exp. Med. 1962; 116:381–406. [PubMed: 14467923]
15. Vazquez-Boland JA, Kuhn M, Berche P, Chakraborty T, Dominguez-Bernal G, Goebel W, Gonzalez-Zorn B, Wehland J, Kreft J. Listeria pathogenesis and molecular virulence determinants. Clin. Microbiol. Rev. 2001; 14:584–640. [PubMed: 11432815]
16. Henry RM, Shaughnessy L, Loessner MJ, Alberti-Segui C, Higgins DE, Swanson JA. Cytolysin-dependent delay of vacuole maturation in macrophages infected with *Listeria monocytogenes*. Cell. Microbiol. 2006; 8:107–119. [PubMed: 16367870]
17. Shaughnessy LM, Hoppe AD, Christensen KA, Swanson JA. Membrane perforations inhibit lysosome fusion by altering pH and calcium in *Listeria monocytogenes* vacuoles. Cell. Microbiol. 2006; 8:781–792. [PubMed: 16611227]
18. Kiderlen AF, Kaufmann SH, Lohmann-Matthes ML. Protection of mice against the intracellular bacterium Listeria monocytogenes by recombinant immune interferon. Eur J Immunol. 1984; 14:964–967. [PubMed: 6436036]
19. Portnoy DA, Schreiber RD, Connelly P, Tilney LG. γ-Interferon limits access of Listeria monocytogenes to the macrophage cytoplasm. J. Exp. Med. 1989; 170:2141–2146. [PubMed: 2511268]
20. Shaughnessy LM, Swanson JA. The role of the activated macrophage in clearing *Listeria monocytogenes* infection. Front Biosci. 2007; 12:2683–2692. [PubMed: 17127272]

21. Myers JT, Tsang AW, Swanson JA. Localized reactive oxygen and nitrogen intermediates inhibit escape of *Listeria monocytogenes* from vacuoles in activated macrophages. J. Immunol. 2003; 171:5447–5453. [PubMed: 14607950]
22. Shiloh M, MacMicking JD, Nicholson S, Brause JE, Potter S, Marino M, Fang F, Dinauer M, Nathan C. Phenotype of mice and macrophages deficient in both phagocyte oxidase and inducible nitric oxide synthase. Immunity. 1999; 10:29–38. [PubMed: 10023768]
23. Davis MJ, Swanson JA. Technical advance: Caspase-1 activation and IL-1β release correlate with the degree of lysosome damage, as illustrated by a novel imaging method to quantify phagolysosome damage. J Leukoc Biol. 2010; 88:813–822. [PubMed: 20587739]
24. Kirkegaard T, Roth AG, Petersen NH, Mahalka AK, Olsen OD, Moilanen I, Zylicz A, Knudsen J, Sandhoff K, Arenz C, Kinnunen PK, Nylandsted J, Jaattela M. Hsp70 stabilizes lysosomes and reverts Niemann-Pick disease-associated lysosomal pathology. Nature. 2010; 463:549–553. [PubMed: 20111001]
25. Nylandsted J, Gyrd-Hansen M, Danielewicz A, Fehrenbacher N, Lademann U, Hoyer-Hansen M, Weber E, Multhoff G, Rohde M, Jaattela M. Heat shock protein 70 promotes cell survival by inhibiting lysosomal membrane permeabilization. J Exp Med. 2004; 200:425–435. [PubMed: 15314073]
26. Dudeja V, Mujumdar N, Phillips P, Chugh R, Borja-Cacho D, Dawra RK, Vickers SM, Saluja AK. Heat shock protein 70 inhibits apoptosis in cancer cells through simultaneous and independent mechanisms. Gastroenterology. 2009; 136:1772–1782. [PubMed: 19208367]
27. Gyrd-Hansen M, Nylandsted J, Jaattela M. Heat shock protein 70 promotes cancer cell viability by safeguarding lysosomal integrity. Cell Cycle. 2004; 3:1484–1485. [PubMed: 15539949]
28. Daugaard M, Kirkegaard-Sorensen T, Ostenfeld MS, Aaboe M, Hoyer-Hansen M, Orntoft TF, Rohde M, Jaattela M. Lens epithelium-derived growth factor is an Hsp70-2 regulated guardian of lysosomal stability in human cancer. Cancer Res. 2007; 67:2559–2567. [PubMed: 17363574]
29. Jinwal UK, Miyata Y, Koren J 3rd, Jones JR, Trotter JH, Chang L, O'Leary J, Morgan D, Lee DC, Shults CL, Rousaki A, Weeber EJ, Zuiderweg ER, Gestwicki JE, Dickey CA. Chemical manipulation of hsp70 ATPase activity regulates tau stability. J Neurosci. 2009; 29:12079–12088. [PubMed: 19793966]
30. Rousaki A, Miyata Y, Jinwal UK, Dickey CA, Gestwicki JE, Zuiderweg ER. Allosteric drugs: the interaction of antitumor compound MKT-077 with human Hsp70 chaperones. J Mol Biol. 2011; 411:614–632. [PubMed: 21708173]
31. Swanson JA. Phorbol esters stimulate macropinocytosis and solute flow through macrophages. J. Cell Sci. 1989; 94:135–142. [PubMed: 2613767]
32. Huotari J, Helenius A. Endosome maturation. EMBO J. 2011; 30:3481–3500. [PubMed: 21878991]
33. Christensen KA, Myers JT, Swanson JA. pH-dependent regulation of lysosomal calcium in macrophages. J. Cell Sci. 2002; 115:599–607. [PubMed: 11861766]
34. Mielke ME, Peters C, Hahn H. Cytokines in the induction and expression of T-cell-mediated granuloma formation and protection in the murine model of listeriosis. Immunol Rev. 1997; 158:79–93. [PubMed: 9314076]
35. Portnoy DA, Jacks PS, Hinrichs DJ. Role of hemolysin for the intracellular growth of Listeria monocytogenes. J. Exp. Med. 1988; 167:1459–1471. [PubMed: 2833557]
36. Beauregard KE, Lee K-D, Collier RJ, Swanson JA. pH-dependent perforation of macrophage phagosomes by listeriolysin O from Listeria monocytogenes. J. Exp. Med. 1997; 186:1159–1163. [PubMed: 9314564]
37. Cassel SL, Eisenbarth SC, Iyer SS, Sadler JJ, Colegio OR, Tephly LA, Carter AB, Rothman PB, Flavell RA, Sutterwala FS. The Nalp3 inflammasome is essential for the development of silicosis. Proc Natl Acad Sci U S A. 2008; 105:9035–9040. [PubMed: 18577586]
38. Hornung V, Bauernfeind F, Halle A, Samstad EO, Kono H, Rock KL, Fitzgerald KA, Latz E. Silica crystals and aluminum salts activate the NALP3 inflammasome through phagosomal destabilization. Nat Immunol. 2008

39. Stuehr DJ, Fasehun OA, Kwon NS, Gross SS, Gonzalez JA, Levi R, Nathan CF. Inhibition of macrophage and endothelial cell nitric oxide synthase by diphenyleneiodonium and its analogs. FASEB J. 1991; 5:98–103. [PubMed: 1703974]
40. O'Donnell BV, Tew DG, Jones OT, England PJ. Studies on the inhibitory mechanism of iodonium compounds with special reference to neutrophil NADPH oxidase. Biochem J. 1993; 290(Pt 1):41–49. [PubMed: 8439298]
41. Li Y, Trush MA. Diphenyleneiodonium, an NAD(P)H oxidase inhibitor, also potently inhibits mitochondrial reactive oxygen species production. Biochem Biophys Res Commun. 1998; 253:295–299. [PubMed: 9878531]
42. Brunk UT, Dalen H, Roberg K, Hellquist HB. Photo-oxidative disruption of lysosomal membranes causes apoptosis of cultured human fibroblasts. Free Radic Biol Med. 1997; 23:616–626. [PubMed: 9215807]
43. Tsan MF, Gao B. Heat shock proteins and immune system. J Leukoc Biol. 2009; 85:905–910. [PubMed: 19276179]
44. Wadhwa R, Sugihara T, Yoshida A, Nomura H, Reddel RR, Simpson R, Maruta H, Kaul SC. Selective toxicity of MKT-077 to cancer cells is mediated by its binding to the hsp70 family protein mot-2 and reactivation of p53 function. Cancer Res. 2000; 60:6818–6821. [PubMed: 11156371]
45. Koren J 3rd, Jinwal UK, Jin Y, O'Leary J, Jones JR, Johnson AG, Blair LJ, Abisambra JF, Chang L, Miyata Y, Cheng AM, Guo J, Cheng JQ, Gestwicki JE, Dickey CA. Facilitating Akt clearance via manipulation of Hsp70 activity and levels. J Biol Chem. 2010; 285:2498–2505. [PubMed: 19889640]
46. Chang L, Miyata Y, Ung PM, Bertelsen EB, McQuade TJ, Carlson HA, Zuiderweg ER, Gestwicki JE. Chemical screens against a reconstituted multiprotein complex: myricetin blocks DnaJ regulation of DnaK through an allosteric mechanism. Chem Biol. 2011; 18:210–221. [PubMed: 21338918]
47. Persson HL, Vainikka LK. TNF-α preserves lysosomal stability in macrophages: a potential defense against oxidative lung injury. Toxicol Lett. 2010; 192:261–267. [PubMed: 19900513]
48. Duewell P, Kono H, Rayner KJ, Sirois CM, Vladimer G, Bauernfeind FG, Abela GS, Franchi L, Nunez G, Schnurr M, Espevik T, Lien E, Fitzgerald KA, Rock KL, Moore KJ, Wright SD, Hornung V, Latz E. NLRP3 inflammasomes are required for atherogenesis and activated by cholesterol crystals. Nature. 2010; 464:1357–1361. [PubMed: 20428172]
49. Boya P, Kroemer G. Lysosomal membrane permeabilization in cell death. Oncogene. 2008; 27:6434–6451. [PubMed: 18955971]
50. Sander LE, Davis MJ, Boekschoten MV, Amsen D, Dascher CC, Ryffel B, Swanson JA, Muller M, Blander JM. Detection of prokaryotic mRNA signifies microbial viability and promotes immunity. Nature. 2011; 474:385–389. [PubMed: 21602824]
51. Elinav E, Strowig T, Henao-Mejia J, Flavell RA. Regulation of the antimicrobial response by NLR proteins. Immunity. 2011; 34:665–679. [PubMed: 21616436]
52. Rock KL, Shen L. Cross-presentation: underlying mechanisms and role in immune surveillance. Immunol Rev. 2005; 207:166–183. [PubMed: 16181335]

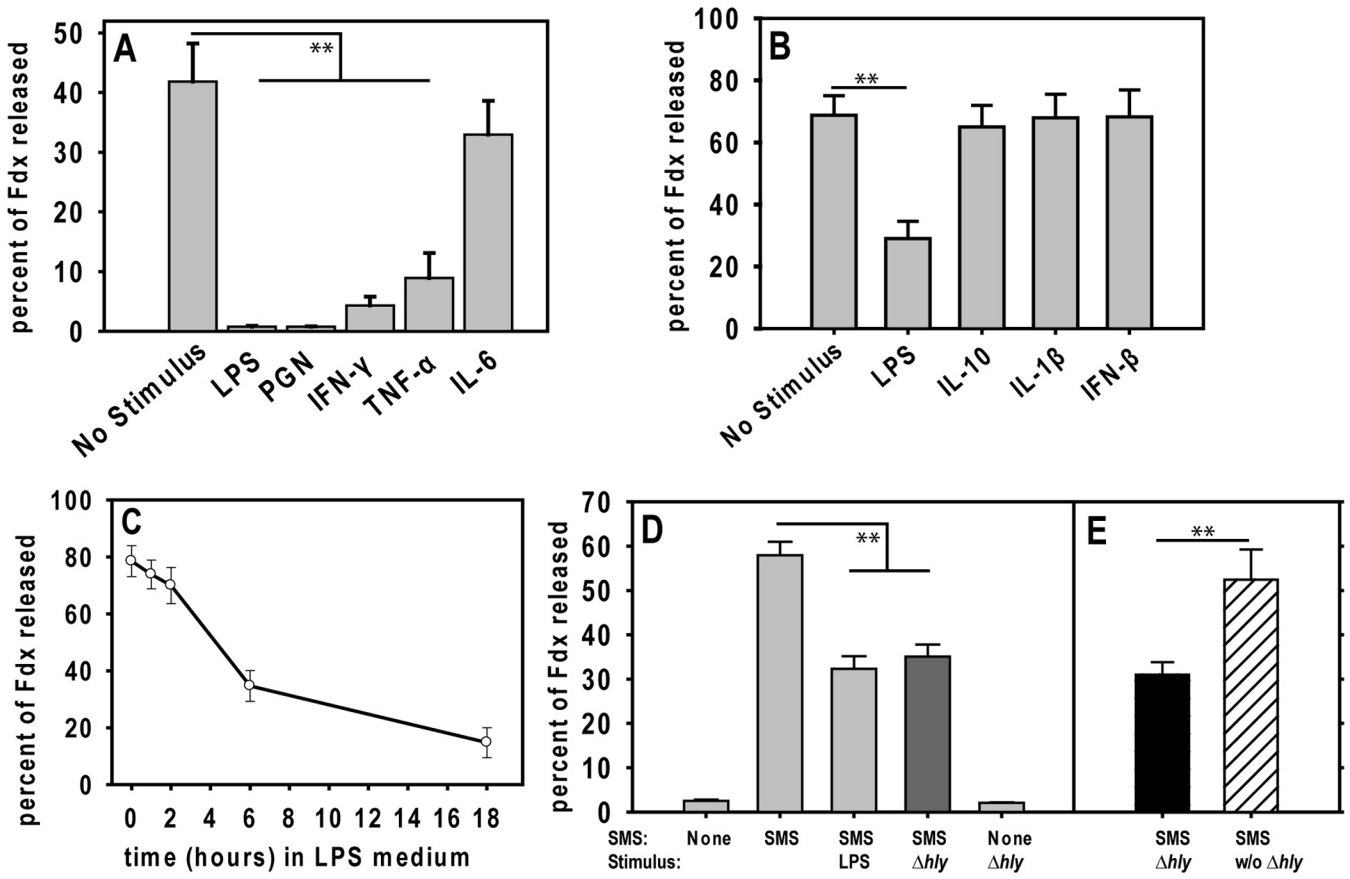

Figure 1. Macrophage activation increases lysosome renitence

(A, B) BMM were loaded with Fdx, chased for 3 hrs in medium without Fdx, then fed SMS and imaged to measure lysosome damage. The number of SMS phagocytosed by each BMM was counted and groups of BMM with similar numbers of SMS phagosomes were compared. LPS, PGN, IFN-γ and TNF-α increased macrophage resistance to damage by SMS; IL-6, IL-10, IL-1β and IFN-β were not protective. Bars and data points are the average percent of Fdx released (±SEM, n ≥ 100 cells). (**C**) Time course of induction by LPS. LPS was included in the medium for the indicated times. BMM stimulated for 18 hrs showed significantly less damage than those stimulated for 0, 1 or 2 hrs ($p<0.001$) or 6 hrs ($p<0.05$); n>30 cells. (**D**) BMM were fed SNARF-1-stained, *hly*-deficient (Δ*hly*) *L.m.*, or stimulated with LPS, then fed 17 hrs later with SMS to measure damage (n>200 cells). Damage was reduced by LPS or by prior infection with Δ*hly L.m.* (**E**) Re-plotted data from the Δ*hly*-induced, SMS-fed condition in D. Using the SNARF-1 fluorescence, BMM were separated into cells which had phagocytosed at least one bacterium (Δ*hly*; dark bar) and those cells in the same coverslips which had not ingested bacteria (w/o Δhly; striped bar). Bars in A-C represent cells which contained 7 – 9 SMS. Bars in D and E represent cells containing 1 – 3 SMS. * = $p<0.05$, ** = $p<0.001$.

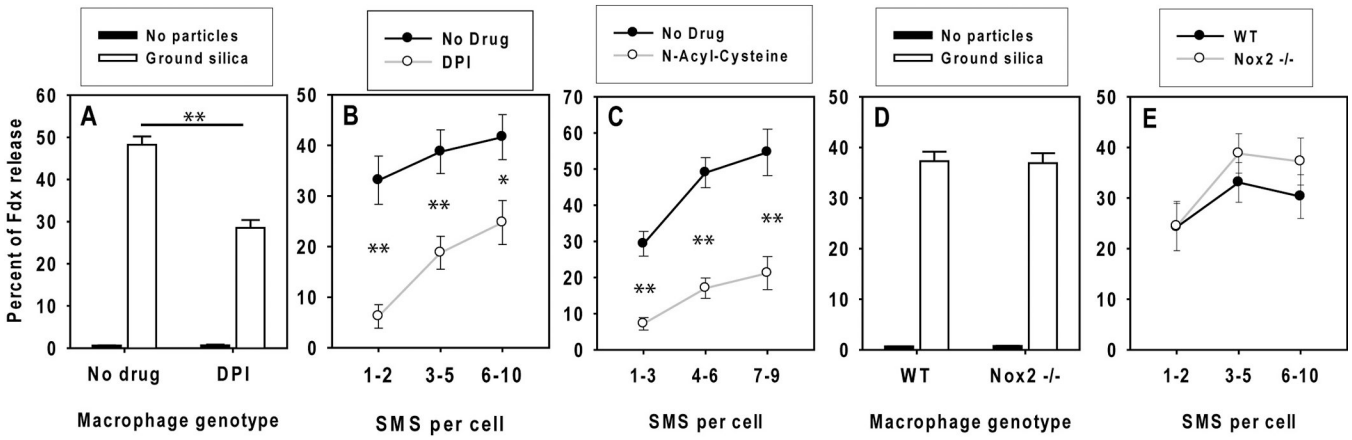

Figure 2. Non-phagosomal reactive oxygen intermediates contribute to silica-mediated lysosome damage

BMM were loaded with Fdx then fed ground silica (**A, D**) or PLL-coated silica microspheres (SMS) (**B, C, E**). 5μM DPI (**A, B**) or 50 mM N-acyl-cysteine (**C**) were added to the medium with the particles. (**D, E**) BMM from wildtype or *Nox2*-deficient (*Nox2* −/−) mice were loaded with Fdx, fed particles and scored for lysosome damage. All data points represent mean ± SEM Fdx release with n>200 BMM for A, B, D and E and n>50 BMM for C. * $p<0.05$, ** $p<0.001$.

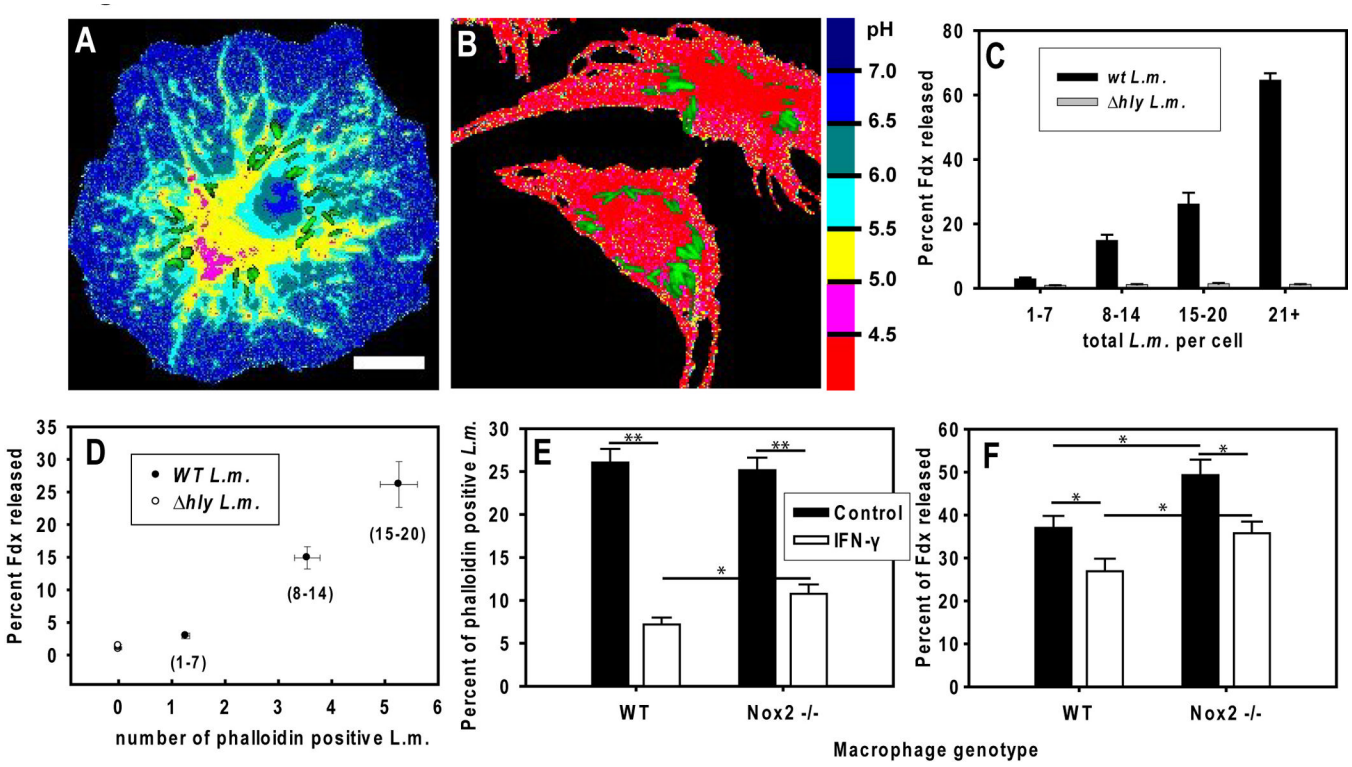

Figure 3. Inducible renitence protects IFN-γ activated macrophages from *L.m.* escape and damage

(**A-C**) Damage by infection with *L.m.* C57/BL6 BMM were loaded with Fdx overnight, chased in dye and antibiotic-free medium for at least 3 hours, infected with SNARF-1-labeled wildtype or Δ*hly L.m.*, chased in gentamicin-containing medium for 90 min, and imaged to measure lysosome damage. (**A**) Fdx pH map of a BMM infected with wildtype *L.m.* Blue pixels indicate lysosome damage (ie., cytoplasmic Fdx). (**B**) Fdx pH map of a BMM infected with Δ*hly L.m.* indicates that the lysosomes are intact. Scale bar = 10 μm. Green pixels in **A** and **B** indicate SNARF-1-labeled *L.m.* (**C**) Average ± SEM percent Fdx release for BMM (n>100 for each group) plotted in groups of cells containing similar numbers of total wildtype (filled bars) or Δ*hly* (open bars) *L.m.* (**D**) Fdx release data re-plotted from C, showing average number of escaped (phalloidin-positive) *L.m.* ± SEM (n>100 for each group) plotted on the x-axis for each category of BMM grouped by total number of *L.m.* per cell (in parentheses). Filled circles represent groups of BMM infected with wildtype *L.m.* while open symbol near the origin represents all groups of Δ*hly L.m.* (**E, F**) C57/BL6 (WT) and *nox2*-deficient (Nox2 −/−) BMM were stimulated with IFN-γ (open bars) or left unstimulated (dark bars) and loaded with Fdx. BMM infected 120 min with wildtype *L.m.* were fixed and stained with phalloidin to measure *L.m.* escape (**E**) or imaged for Fdx release (**F**). Bars in **E** are average percent of phalloidin-positive *L.m.* and error bars are SEM (n ≥350 cells). Bars in **F** indicate average percent of Fdx released ± SEM of BMM containing 1–7 *L.m.*, per cell (n ≥130 cells). * p<0.05 ** p<0.001

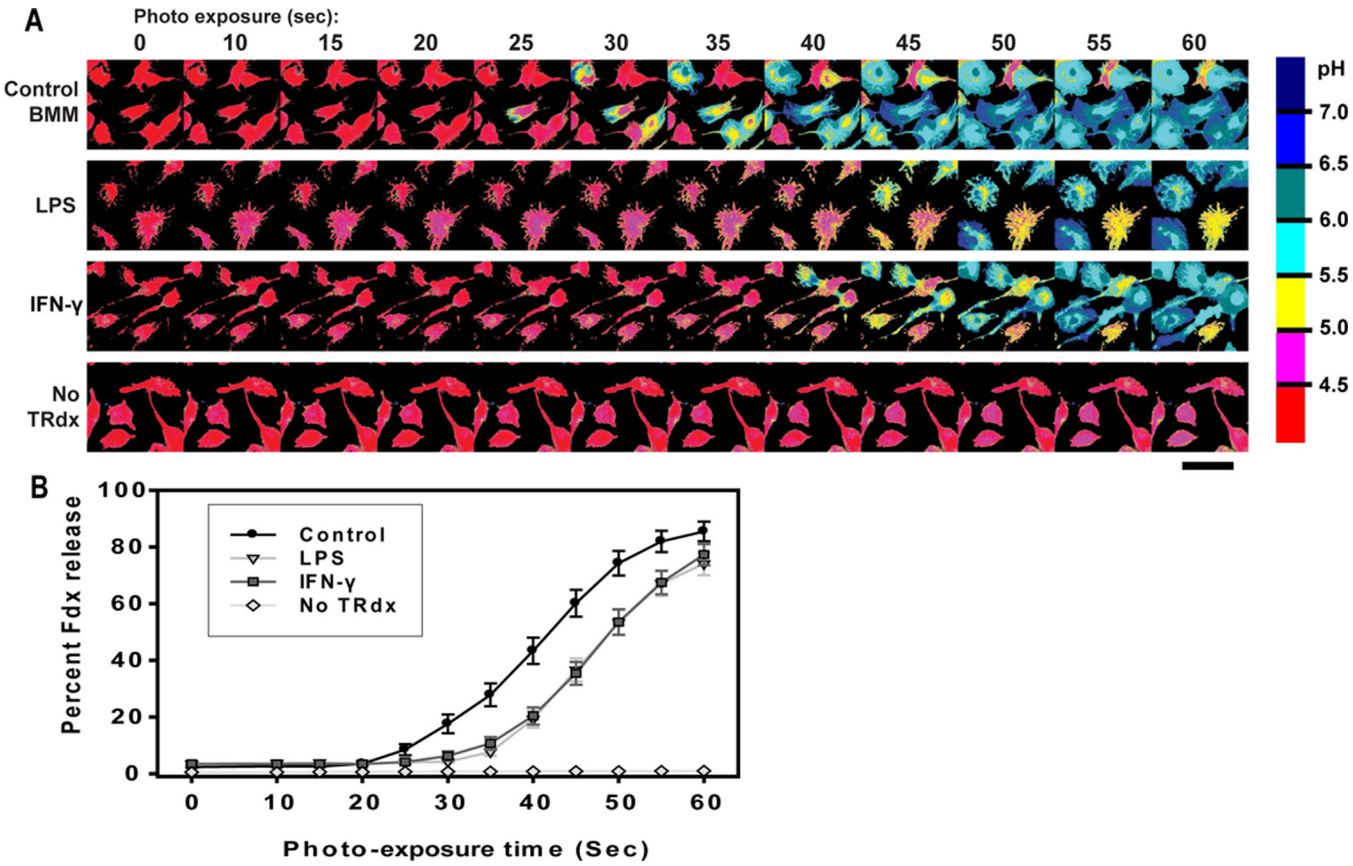

Figure 4. Inducible renitence protects against photodamage

BMM lysosomes were loaded with Fdx and TRdx. Cells were exposed to 580 nm light from the microscope arc lamp in 5-sec pulses; Fdx pH images were acquired between each pulse. (**A**) Sample pH maps of fields of photostimulated BMM, with pH color key on the right and a 50 μm scale bar below images (right side). (**B**) Percent of Fdx released was calculated for each cell. Average percent release for each time point is plotted ± SEM. At least 50 cells were analyzed for each condition. Control macrophages were significantly different from both LPS and IFN-γ simulated cells with $p<0.001$ for all data between 30 to 50 sec and $p<0.05$ for the data at 25 and 55 sec (un-paired Student's T-test).

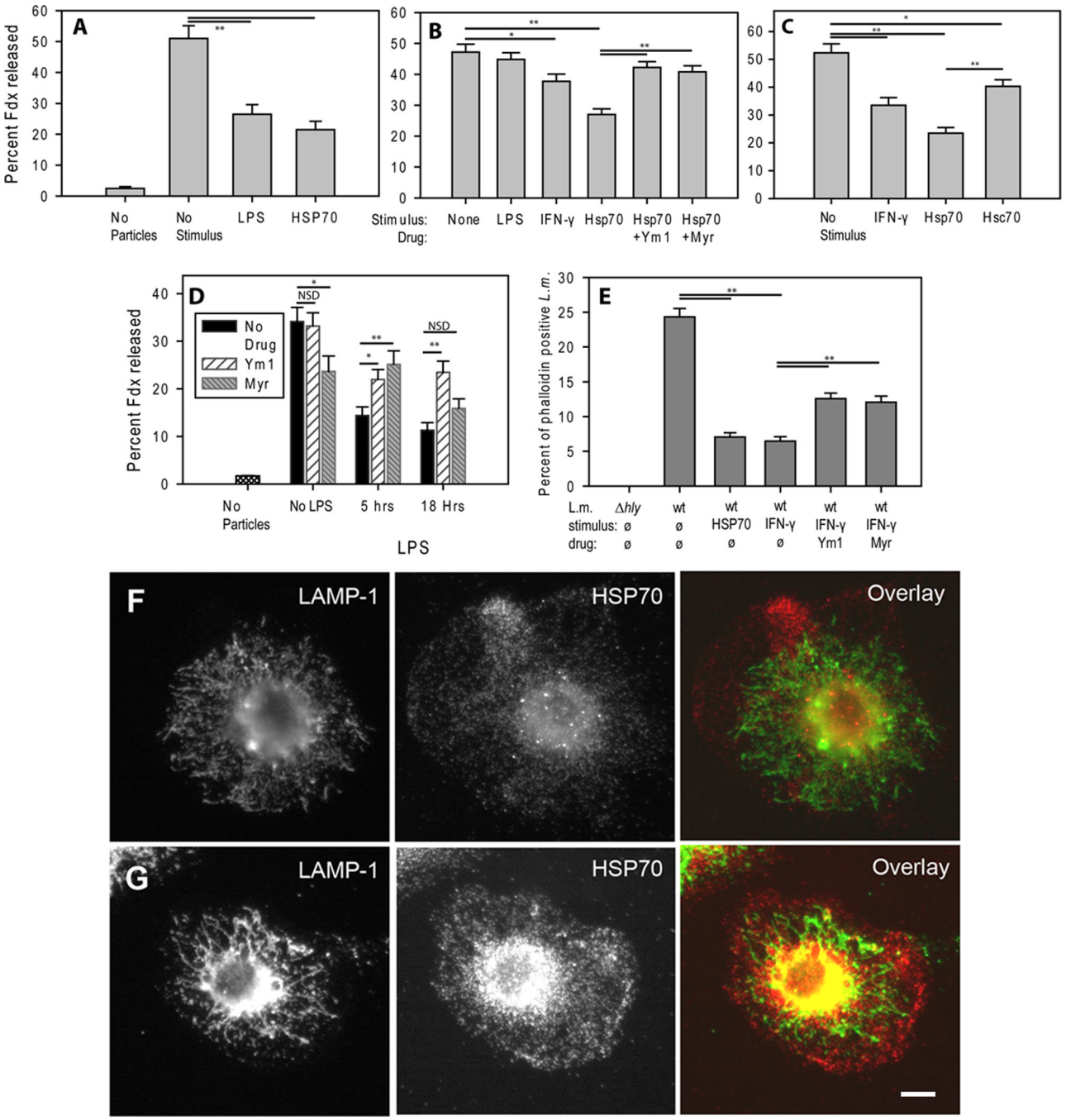

Figure 5. HSP70 contributes to inducible renitence

(A-D) HSP70 inhibits damage by SMS. (**A**) Fdx-loaded BMM were exposed to LPS or 300 nM recombinant HSP70 for 5 hrs, then cells were rinsed and fed SMS for 1 hr and imaged for Fdx release (1–3 SMS/cell, n>100 cells). (**B**) BMM from TLR4−/− mice were exposed to IFN-γ overnight, LPS for 5 hrs or 300 nM HSP70 for 5 hrs, with or without HSP70 inhibitors Ym1 (20 μM) or Myr (25 μM). HSP70 inhibited lysosome damage (n>300 cells). (**C**) TLR4−/− BMM were exposed to IFN-γ overnight or 300 nM recombinant HSP70 or HSC70 for 5 hrs, then assayed for SMS damage (n>180 cells). (**D**) Wildtype BMM were exposed to LPS for 5 or 18 hrs or left untreated. Ym1 (20 μM) or Myr (25 μM) were

included for the last 5 hrs of stimulation (n>120 cells). (**E**) TLR4−/− BMM were exposed to recombinant HSP70 for 5 hrs or to IFN-γ overnight. Indicated IFN-γ-stimulated cells were also incubated with Ym1 or Myr for the last 5 hrs of stimulation. BMM were infected with *wt*, or Δ*hly L.m.* and vacuolar escape was measured (n>500 cells). Bars are population averages (± SEM). * $p<0.05$, ** $p<0.001$. (F, G) Immunofluorescence localization of HSP70 and LAMP-1 in (F) unstimulated BMM and (G) IFN-γ-stimulated BMM. Overlay images show corresponding distributions of LAMP-1 (green) and Hsp70 (red). Scale bar = 10 μm.